Available online at www.sciencedirect.com
SCIENCE DIRECT®
International Journal of Heat and Fluid Flow 26 (2005) 1–11
International Journal of HEAT AND FLUID FLOW
www.elsevier.com/locate/ijhff

Turbulent mixed convection from a large, high temperature, vertical flat surface

G. Evans [a,*], R. Greif [b], D. Siebers [a], S. Tieszen [c]

[a] Sandia National Laboratories [1], P.O. Box 969, Livermore, CA 94551-0969, USA
[b] Department of Mechanical Engineering, University of California, Berkeley, CA 94720-1740, USA
[c] Sandia National Laboratories, P.O. Box 5800 MS1135, Albuquerque, NM 87185, USA

Received 21 February 2004; accepted 10 July 2004
Available online 27 August 2004

Abstract

Turbulent mixed convection heat transfer at high temperatures and large length scales is an important and seldom studied phenomenon that can represent a significant part of the overall heat transfer in applications ranging from solar central receivers to objects in fires. This work is part of a study to validate turbulence models for predicting heat transfer to or from surfaces at large temperature differences and large length scales. Here, turbulent, three-dimensional, mixed convection heat transfer in air from a large (3 m square) vertical flat surface at high temperatures is studied using two RANS turbulence models: a standard k–ε model and the $\overline{v^2}$–f model. Predictions for three cases spanning the range of the experiment (Siebers, D.L., Schwind, R.G., Moffat, R.F., 1982. Experimental mixed convection from a large, vertical plate in a horizontal flow. Paper MC13, vol. 3, Proc. 7th Int. Heat Transfer Conf., Munich; Siebers, D.L., 1983. Experimental mixed convection heat transfer from a large, vertical surface in a horizontal flow. PhD thesis, Stanford University) from forced ($Gr_H/Re_L^2 = 0.18$) to mixed ($Gr_H/Re_L^2 = 3.06$) to natural ($Gr_H/Re_L^2 = \infty$) convection are compared with data. The results show a decrease in the heat transfer coefficient as Gr_H/Re_L^2 is increased from 0.18 to 3.06, for a free-stream velocity of 4.4 m/s. In the natural convection case, the experimental heat transfer coefficient is approximately constant in the fully turbulent region, whereas the calculated heat transfer coefficients show a slight increase with height. For the three cases studied, the calculated and experimental heat transfer coefficients agree to within 5–35% over most of the surface with the $\overline{v^2}$–f model results showing better agreement with the data. Calculated temperature and velocity profiles show good agreement with the data.

Keywords: Turbulent mixed convection; RANS; $\overline{v^2}$–f; k–ε; Vertical flat plate

1. Introduction

The present work is a study of turbulent, three-dimensional, mixed convection over a large (3 m square), vertical flat surface at high temperatures (cf. Fig. 1). Siebers et al. (1985) described an experimental facility and presented experimental results for variable property natural convection for this surface in air. Siebers et al. (1982, 1983) also presented experimental results for forced and mixed convection and these data are studied in this work to validate the $\overline{v^2}$–f and standard k–ε turbulence models for these conditions. The range of the mixed convection parameter Gr_H/Re_L^2 (where H is the height and L is the horizontal length of the surface) covered in these experiments was from 0.1 to 30.23, i.e., from forced to mixed to natural convection; the surface temperature was as high as 588 °C. The range of conditions (Gr_H to 2×10^{12}; Re_L to 2×10^6; $Pr = 0.7$)

* Corresponding author. Tel.: +1 925 294 2795.
E-mail address: evans@sandia.gov (G. Evans).
[1] Sandia is a multiprogram laboratory operated by Sandia Corporation, a Lockheed Martin Company, for the United States Department of Energy's National Nuclear Security Administration under Contract DE-AC04-94-AL85000.

0142-727X/$ - see front matter © 2004 Elsevier Inc. All rights reserved.
doi:10.1016/j.ijheatfluidflow.2004.07.001

Nomenclature

Gr_H	Grashof number = $g\beta(T_w - T_\infty)H^3/\nu_\infty^2$
H	height of surface
L	horizontal length of surface, length scale in f equation
Pr	Prandtl number = $c_p\mu/k$
Pr_t	turbulent Prandtl number = $c_p\mu_t/k_t = 0.9$
Re_L	Reynolds number = $u_\infty L/\nu_\infty$
T	temperature, time scale in $\overline{v^2}$–f model
c_p	constant pressure specific heat
f	$\overline{v^2}$–f model variable related to pressure strain correlation, accounting for wall blockage
g	acceleration of gravity
h	enthalpy, heat transfer coefficient
k	turbulent kinetic energy, thermal conductivity
p	pressure
t	time
u	horizontal component of velocity
u_τ	wall shear velocity = $\sqrt{\tau_w/\rho}$, approximated here with $C_\mu^{1/4}k^{1/2}$
v	vertical component of velocity
$\overline{v^2}$	$\overline{v^2}$–f model variable related to component of turbulent kinetic energy normal to surface
w	component of velocity normal to surface
x	horizontal coordinate
y	vertical coordinate
z	coordinate normal to surface
β	coefficient of thermal expansion = $1/T_\infty$
ε	turbulence dissipation rate
μ	dynamic viscosity
μ_t	turbulent viscosity
ν	kinematic viscosity = μ/ρ
ρ	density
τ	shear stress

Subscripts

∞	freestream conditions far from surface
w	surface conditions
t	turbulent quantity

Superscript

+	non-dimensional quantity using wall scaling

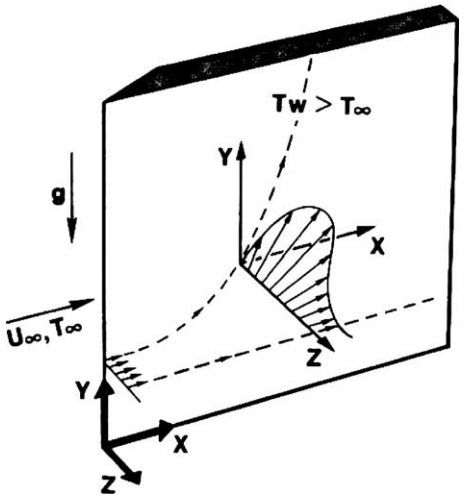

Fig. 1. Geometry and coordinate system.

covers complex phenomena including large effects of variable properties on the heat transfer due to the large temperature differences between the heated surface and the ambient air and three-dimensional flow as a result of the buoyancy force being at a 90° angle to the horizontal forced flow over the surface. Siebers found that the heat transfer could be characterized as mixed convection, defined to be the condition when the average heat transfer differed by more than 5% from either forced convection or natural convection acting alone, when Gr_H/Re_L^2 was between 0.7 and 10.

Afshari (1989) applied a boundary layer formulation to mixed convection with applications to Siebers' experiment. A mixing length model was applied to approximate the three-dimensional, turbulent, mixed convection transport. In a series of experimental and theoretical publications, Armaly et al. (2000), Abu-Mulaweh et al. (2000, 2001), Li et al. (1998), Ramachandran et al. (1990), and Chen et al. (1987) have studied turbulent mixed and natural convection in external flows. Their work has covered horizontal, inclined, and vertical surfaces as well as backward facing step flows. Kitamura and Inagaki (1987) and Hattori et al. (2000, 2001) have carried out experimental studies of mixed convection along a vertical surface with emphasis on the laminarization process of the boundary layer due to free-stream effects. Seo and Parameswaran (2000) studied the effect of buoyancy on turbulent flow and heat transfer in a vertical backward-facing step flow with a k–ε turbulence model. Humphrey and To (1986) studied turbulent mixed convection in a heated cavity using a k–ε turbulence model. With the exception of Afshari's boundary layer analysis of Siebers' experiment, the studies mentioned above are two-dimensional. Most of the work has been for moderate temperature differences, exceptions being the analyses of Afshari and Humphrey and To.

The current study is a three-dimensional, elliptic analysis of the turbulent, variable property mixed convection flow and heat transfer of air over a heated vertical surface. Our application is to turbulent mixed

convection at high temperatures and large length scales. The turbulence is modeled using a Reynolds averaged Navier–Stokes (RANS) approach. Specifically two turbulence models were used to determine the local heat transfer and fluid flow: the standard k–ε model (Jones and Launder, 1972; Launder and Spalding, 1974) and the $\overline{v^2}$–f model (Durbin, 1991, 1993). In a study of the heat transfer from a heated pedestal to an impinging jet flow, Behnia et al. (1999) showed that predictions using the $\overline{v^2}$–f model were significantly better than the results from a widely used low Reynolds number k–ε model. In the present work the $\overline{v^2}$–f model and the standard k–ε model are evaluated for a simpler geometry but for conditions of strong buoyancy, large temperature differences, and large length scales. This study represents the first time that the $\overline{v^2}$–f model is utilized to study turbulent mixed convection.

2. Description of numerical formulation

The computer code, Fuego, described in Moen et al. (2002), is used in this study to solve the three-dimensional, turbulent, low Mach number, Reynolds averaged equations of Newtonian fluid flow with heat transfer. It is pointed out that the formulation includes variable properties; the Boussinesq approximation is not used. A control volume finite element method of discretization (unstructured grid methodology) of the conservation equations is used in which the dependent variables are co-located at the nodes of the elements. A control volume, shown in 2D for simplicity along with the elements that make up the control volume, is shown in Fig. 2 where the x denotes location of flux evaluation.

In integral form, the conservation equations are given by:

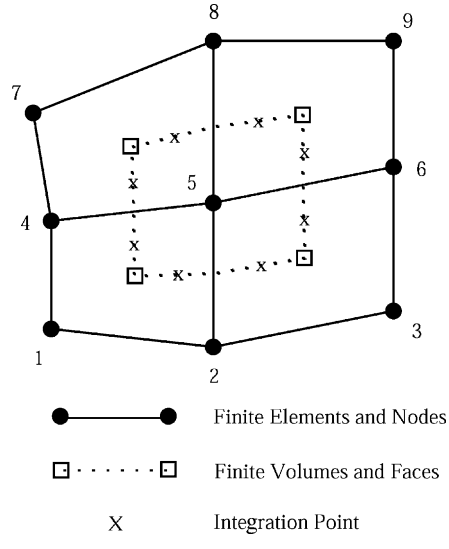

Fig. 2. Discretization scheme showing control volume and elements (in 2D); control volume is centered about node 5.

conservation of mass:

$$\int \frac{\partial \rho}{\partial t}\,\mathrm{d}V + \int \rho u_j n_j\,\mathrm{d}S = 0, \tag{1}$$

conservation of momentum:

$$\int \frac{\partial \rho u_i}{\partial t}\,\mathrm{d}V + \int (\rho u_i u_j + p\delta_{ij}) n_j\,\mathrm{d}S = \int (\mu + \mu_\mathrm{t})\left(\frac{\partial u_i}{\partial x_j} + \frac{\partial u_j}{\partial x_i}\right) n_j\,\mathrm{d}S + \int (\rho - \rho_\infty) g_i\,\mathrm{d}V, \tag{2}$$

conservation of energy:

$$\int \frac{\partial \rho h}{\partial t}\,\mathrm{d}V + \int \rho h u_j n_j\,\mathrm{d}S = \int \left(\frac{\mu}{Pr} + \frac{\mu_\mathrm{t}}{Pr_\mathrm{t}}\right)\frac{\partial h}{\partial x_j} n_j\,\mathrm{d}S. \tag{3}$$

The k–ε model equations are given by

$$\int \frac{\partial \rho k}{\partial t}\,\mathrm{d}V + \int \rho k u_j n_j\,\mathrm{d}S = \int \mu_\mathrm{t}\frac{\partial k}{\partial x_j} n_j\,\mathrm{d}S + \int (P_k - \rho\varepsilon)\,\mathrm{d}V, \tag{4}$$

$$\int \frac{\partial \rho \varepsilon}{\partial t}\,\mathrm{d}V + \int \rho \varepsilon u_j n_j\,\mathrm{d}S = \int \frac{\mu_\mathrm{t}}{\sigma_\varepsilon}\frac{\partial \varepsilon}{\partial x_j} n_j\,\mathrm{d}S + \int \frac{\varepsilon}{k}(C_{\varepsilon_1} P_k - C_{\varepsilon_2}\rho\varepsilon)\,\mathrm{d}V. \tag{5}$$

The $\overline{v^2}$–f model equations are given by

$$\int \frac{\partial \rho k}{\partial t}\,\mathrm{d}V + \int \rho k u_j n_j\,\mathrm{d}S = \int (\mu + \mu_\mathrm{t})\frac{\partial k}{\partial x_j} n_j\,\mathrm{d}S + \int (P_k - \rho\varepsilon)\,\mathrm{d}V, \tag{6}$$

$$\int \frac{\partial \rho \varepsilon}{\partial t}\,\mathrm{d}V + \int \rho \varepsilon u_j n_j\,\mathrm{d}S = \int \left(\mu + \frac{\mu_\mathrm{t}}{\sigma_\varepsilon}\right)\frac{\partial \varepsilon}{\partial x_j} n_j\,\mathrm{d}S + \int \frac{(C'_{\varepsilon_1} P_k - C_{\varepsilon_2}\rho\varepsilon)}{T}\,\mathrm{d}V, \tag{7}$$

$$\frac{\partial \rho \overline{v^2}}{\partial t}\,\mathrm{d}V + \int \rho \overline{v^2} u_j n_j\,\mathrm{d}S = \int (\mu + \mu_\mathrm{t})\frac{\partial \overline{v^2}}{\partial x_j} n_j\,\mathrm{d}S + \int \left(\rho k f - \frac{\rho N \overline{v^2}}{T_1}\right)\mathrm{d}V, \tag{8}$$

$$\int \frac{f}{L^2}\,\mathrm{d}V - \int \frac{\partial f}{\partial x_j} n_j\,\mathrm{d}S = \int \frac{C_1}{L^2}\frac{(2/3 - \overline{v^2}/k)}{T_1}\,\mathrm{d}V + \int \frac{C_2}{L^2}\frac{P_k}{\rho k}\,\mathrm{d}V + \int \frac{(N-1)}{L^2}\frac{\overline{v^2}/k}{T_1}\,\mathrm{d}V. \tag{9}$$

The turbulent Prandtl number, Pr_t, is set to 0.9. In the k–ε model the turbulent viscosity is given by

$$\mu_t = C_\mu \rho \frac{k^2}{\varepsilon}, \tag{10}$$

whereas in the $\overline{v^2}$–f model the turbulent viscosity is given by

$$\mu_t = C_\mu \rho \overline{v^2} T. \tag{11}$$

The production of turbulent kinetic energy P_k is given by

$$P_k = 2\mu_t S^2, \tag{12}$$

where

$$S^2 = \frac{1}{4}\left(\frac{\partial u_i}{\partial x_j} + \frac{\partial u_j}{\partial x_i}\right)\left(\frac{\partial u_i}{\partial x_j} + \frac{\partial u_j}{\partial x_i}\right). \tag{13}$$

In the $\overline{v^2}$–f model the time and length scales and the coefficient of production in the dissipation Eq. (7) are given by

$$T_1 = \max\left[\frac{k}{\varepsilon}, 6\sqrt{\frac{v}{\varepsilon}}\right] \quad T = \min\left[T_1, \frac{\alpha}{2\sqrt{3}}\frac{k}{\overline{v^2} C_\mu \sqrt{S^2}}\right] \tag{14}$$

and

$$L = C_L \max\left[\frac{k^{3/2}}{\varepsilon}, C_\eta\left(\frac{v^3}{\varepsilon}\right)^{1/4}\right], \tag{15}$$

$$C'_{\varepsilon_1} = C_{\varepsilon_1}\left(1 + 0.045\sqrt{\frac{k}{\overline{v^2}}}\right). \tag{16}$$

The constants in the k–ε model are

$$C_\mu = 0.09; \quad \sigma_\varepsilon = 1.3; \quad C_{\varepsilon_1} = 1.45; \quad C_{\varepsilon_2} = 1.92 \tag{17}$$

and in the $\overline{v^2}$–f model the constants are

$$\begin{aligned} &C_\mu = 0.22; \quad \sigma_\varepsilon = 1.3; \quad C_{\varepsilon_1} = 1.4; \quad C_{\varepsilon_2} = 1.9; \\ &C_1 = 0.4; C_2 = 0.3; \\ &N = 6; \quad C_L = 0.23; \quad C_\eta = 70; \quad \alpha = 0.6. \end{aligned} \tag{18}$$

For greater numerical stability, the formulation of the $\overline{v^2}$–f model given here differs from the model recommended by Durbin (2003) in two respects: first, the realizability constraint (Durbin, 1996) given in the time scale (14) is not used in the equation for f (i.e., T_1 is used in Eq. (9) instead of T), and second, T_1 replaces k/ε in the sink term in the last integral on the right hand side of the $\overline{v^2}$ Eq. (8). The second change was shown by Sveningsson (2003) to result in improved convergence and proper far field behavior of $\overline{v^2}$ in stagnation flow.

In Fuego, the equations are solved in a segregated manner using a semi-implicit scheme in which the control volume mass fluxes are evaluated from the solution at the previous iteration. A first-order upwind method was used for the convection terms in which the convected quantity is determined using the value at the adjacent node upstream of the integration point (cf. Fig. 2). The steady-state result was approached via time marching with a CFL condition (maximum nodal CFL number) of approximately 10. For numerical stability, under-relaxation factors of approximately 0.5 were applied to the turbulence quantities and enthalpy. Pressure and momentum variables were not under-relaxed. The non-linear residuals of the equations were reduced by 6–12 orders of magnitude, depending on the variable, and all results presented were converged to a steady state, after which continued iteration resulted in negligible changes in the results.

3. Boundary conditions

The modeled domain consisted of a rectangular parallelepiped region adjacent to the vertical surface ($L = 2.95$ m, $H = 3.03$ m, in the x (horizontal) and y (vertical) coordinate directions, respectively; cf. Fig. 1), extending outward from the surface in the z direction for 1.12 m. This distance is sufficiently large so that the results are independent of this dimension (see discussion of results section). At the vertical leading edge of the surface ($x = 0$) the measured free-stream velocity is applied uniformly. For the forced and mixed convection cases (identified as ID604 and ID648, respectively, in Siebers, 1983), the inlet values of turbulence intensity and length scale were set to 3% and 0.1 m, respectively. For ID604, this corresponded to inlet turbulence quantities of k, ε, and $\overline{v^2}$ of 261.4 cm^2/s^2, 422.5 cm^2/s^3, and 174.2 cm^2/s^2, respectively. For ID648, this corresponded to inlet turbulence quantities of k, ε, and $\overline{v^2}$ of 250 cm^2/s^2, 394 cm^2/s^3, and 166 cm^2/s^2, respectively. For the natural convection case (ID643 in Siebers, 1983) a low level of turbulence was set for fluid that was entrained across any open boundary; specifically, entrained levels of k, ε, and $\overline{v^2}$ were 1.5 cm^2/s^2, 0.037 cm^2/s^3, and 1.0 cm^2/s^2, respectively. At all other open boundaries (vertical trailing edge at $x = L$, horizontal leading and trailing edges at $y = 0$ and $y = H$, respectively, and free-stream boundary at $z = 1.12$ m), a pressure boundary condition, $p = 0$, is applied. The momentum and energy equations are solved at open boundaries. If the flow is entering the domain the temperature on the boundary is given by the free stream value.

For the $\overline{v^2}$–f model, the no-slip boundary condition is applied on the surface. The 105 measured surface temperatures (Siebers, 1983) are used as the thermal boundary condition. Values of the surface temperature at intermediate points on the surface are obtained by bilinear interpolation. The boundary conditions for the turbulence quantities at the surface are given by

$$k = \overline{v^2} = f = 0; \quad \varepsilon = 2\nu\frac{k_1}{z_1^2}, \tag{19}$$

where k_1 and z_1 are the turbulent kinetic energy and normal distance from the surface, respectively, of the first node away from the surface.

For the k–ε model, wall functions are used for the control volumes associated with nodes on the wall (surface). Fig. 3 shows a simplified wall-adjacent 2D element and a wall node P along with one of the sub-control volumes (scv) associated with that node.

The momentum conservation equation for the component of momentum parallel to the wall is solved for the control volume associated with node P (part of which is shown as scv in Fig. 3). A flux of variable Φ (e.g., u or k), $\rho u\Phi$, is shown at one of the sub-control volume faces. The value of Φ is obtained from the nearest upstream node (e.g., u_{P_u} or k_{P_u} shown in Fig. 3). The law of the wall is applied to give the shear stress, τ_w, on the wall face of the scv:

$$\tau_w = \frac{\rho C_\mu^{1/4} k_p^{1/2} \kappa}{\ln\left(E z_p^+\right)} u_p, \tag{20}$$

where $\kappa = 0.42$; $E = 9.8$ and

$$z_p^+ = \frac{z_p C_\mu^{1/4} k_p^{1/2}}{\nu} \tag{21}$$

and z_p is the normal distance from the wall to the center of the scv and now subscript p refers to quantities evaluated at the wall node P. Using the thermal law of the wall the heat flux applied to the wall face of the scv is given by

$$q_w = \frac{\rho c_p (T_w - T_p) C_\mu^{1/4} k_p^{1/2} \kappa}{Pr_t \ln\left(E z_p^+\right)}, \tag{22}$$

where T_p is the calculated temperature at the wall node P which represents the temperature of the near-wall control volume (part of which is shown in Fig. 3 as scv), and T_w is the measured (or linearly interpolated from the measurements) wall temperature.

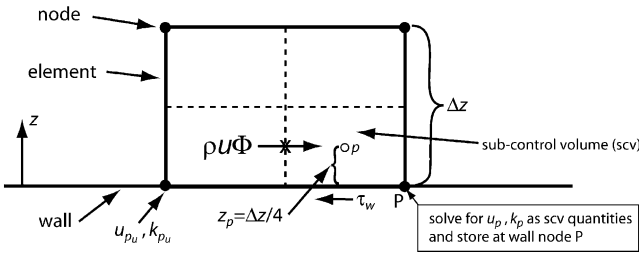

Fig. 3. Simplified 2D wall-adjacent element with wall node P and part of the control volume (scv) associated with P.

The production and dissipation terms in the turbulent kinetic energy equation are altered in the control volume adjacent to the wall to be

$$P_k = \frac{\rho C_\mu^{3/4} k_p^{3/2}}{\kappa z_p}, \tag{23}$$

$$\rho\varepsilon = \frac{\rho u_\tau^3}{\kappa z_p} = \frac{\rho C_\mu^{3/4} k_p^{3/2}}{\kappa z_p} \tag{24}$$

which simply states that production and dissipation of turbulent kinetic energy are in balance. With these modifications to the k equation along with the neglect of diffusion of turbulent kinetic energy across the wall face of the scv, the equation for k is solved for the near-wall control volume to give a value of k at the wall node P. The boundary condition at the wall for the ε equation is a Dirichlet condition given by

$$\varepsilon_p = \frac{u_\tau^3}{\kappa z_p} = \frac{C_\mu^{3/4} k_p^{3/2}}{\kappa z_p}. \tag{25}$$

Air is modeled as a uniform mixture of nitrogen and oxygen with mole fractions of 0.7905 and 0.2095, respectively. The temperature dependent properties of this mixture are evaluated using the local node temperature with the CHEMKIN-III (Kee et al., 1996) and associated transport package (Kee et al., 1991) software, thus fully capturing the effects of variable fluid properties.

The local heat transfer coefficient, h, is defined as

$$h = q_w/(T_w - T_\infty) = -k\left.\frac{\partial T}{\partial z}\right|_{z=0} \Big/ (T_w - T_\infty) \tag{26}$$

for the $\overline{v^2}$–f model, and Eq. (22) is used for the k–ε model (where the coordinate normal to the surface is z in this study).

4. Discussion of results

The parameter range covered in the experiment is shown in Fig. 4. Here Gr_H is the Grashof number based on the height H of the vertical surface and Re_L is the Reynolds number based on the length L of the surface in the horizontal (x coordinate) direction. In both parameters, the properties (experiment is for air) are evaluated at the free-stream temperature T_∞. Prior to Siebers' experimental study, the data relevant to this problem are shown by the gray shaded region in Fig. 4; all the earlier data in the natural convection region at high Gr_H were for temperatures below 150 °C. Thus the effects of significant property variations on the heat transfer in turbulent natural and mixed convection were shown for the first time by Siebers (1983). The cases studied here are identified on the figure and cover the limiting conditions of the experiment.

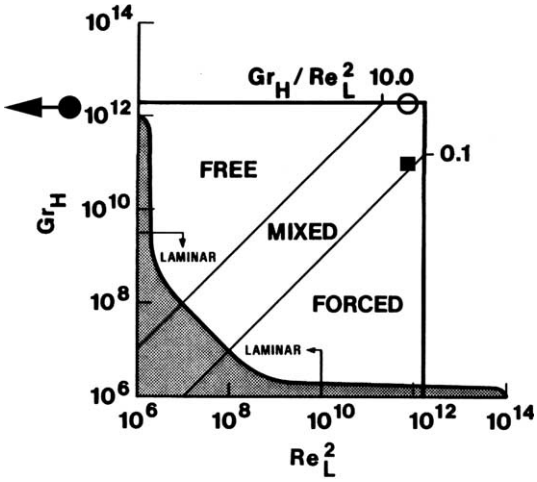

Fig. 4. Parameter range of Siebers' experiment (gray shaded region shows parameter range prior to Siebers' experiment) and the three cases simulated in this study (square is forced convection case, ID604; filled circle is natural convection case, ID643, where the arrow indicates this case is for $Re = 0$; open circle is mixed convection case, ID648).

4.1. Forced convection ($Gr_H/Re_L^2 = 1.4 \times 10^{11}/(8.9 \times 10^5)^2 = 0.18$)

For the forced convection condition the results for the heat transfer coefficient, h, are shown in Fig. 5. The free-stream (and inlet at $x = 0$) velocity and temperature are 4.4 m/s and 289 K, respectively; the average surface temperature is 323 K. The data of Siebers (1983) with error bars included and results of both the $\overline{v^2}$–f and the k–ε turbulence models are presented. For this experimental condition a trip wire was located 0.65 m ($Re_x = 1.9 \times 10^5$) downstream of the vertical leading edge ($x = 0$) of the surface. Correspondingly, the data show an initial decrease in h up to the location of the trip wire, followed by an increase of h and then a gradual decline. This corresponds to an initial decrease in h for a thickening laminar boundary layer followed by transition to a turbulent boundary layer with subsequent thickening and a gradual decline in h. Calculations with both models are made assuming a turbulent flow and a uniform velocity profile at the leading edge of the surface. Results of both models agree qualitatively with the data; that is, they show an initial decrease in h followed by an increase of h and then a gradual decline. Even though neither model has a transition criterion and the effect of the trip wire was not accounted for in the models, the results of both models do show a transition-like behavior (i.e., a decrease followed by an increase in the heat transfer). The k–ε model shows this behavior occurring from approximately 0.75 m < x < 2 m. The $\overline{v^2}$–f model exhibits this behavior upstream and in the vicinity of the trip wire. The transition-like behavior of the results may be due to the adjustment of the flow to the no-slip condition on the surface; however it was not the intention of this work to study transition or the effects of velocity profile or turbulence level on the transition phenomenon.

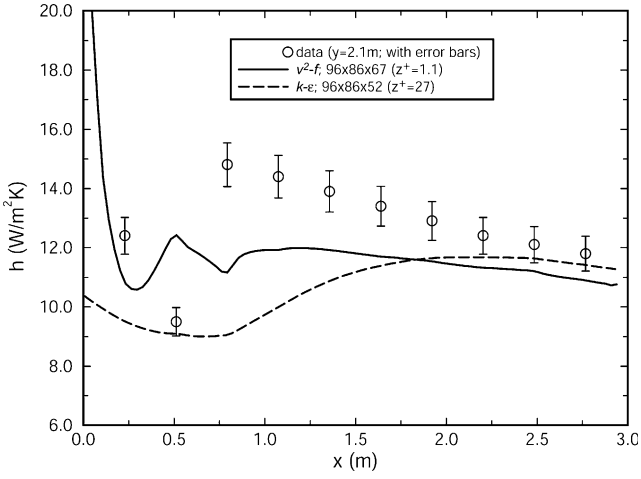

Fig. 5. Variation of local heat transfer coefficient in x direction at vertical position on surface of $y = 2.1$ m; forced convection (ID604); $Gr_H/Re_L^2 = 0.18$; $u_\infty = 4.4$ m/s; $T_{w_{avg}} = 323$ K.

Downstream of the trip wire, both models under-predict the data; e.g., at $x = 1.75$ m, the data are under-predicted by approximately 12%. In the boundary layer study of Afshari (1989), the beginning and end of transition were required to occur at the locations shown in the data of Siebers (1983) and very good agreement with the data was obtained.

The sensitivity of the numerical results to mesh spacing has been determined. For the $\overline{v^2}$–f model, the results shown were computed on a $96 \times 86 \times 67$ mesh in the (x, y, z) coordinate directions, respectively, with $z^+ \approx 1$. Results (not shown) of the local heat transfer computed on a $125 \times 112 \times 87$ mesh with $z^+ \approx 2$ differed by less than 1%. For the k–ε model the results shown were computed on a $96 \times 86 \times 52$ mesh with $z^+ \approx 27$. Results (not shown) of the local heat transfer computed on a $67 \times 60 \times 36$ mesh with $z^+ \approx 27$ differed by less than 1%. It is also emphasized that additional mesh studies have been carried out and verify the mesh insensitivity of the results for the three cases studied. The sensitivity of the results to the size of the domain in the z direction was checked; negligible differences were found for a domain of 0.8 m compared with the results shown here where the domain was 1.12 m. Temperature and velocity profiles at $x = 1.64$ m, $y = 1.95$ m, are compared with the experimental data in Figs. 6 and 7, respectively. There is good agreement between the data and the results of both turbulence models. Profiles at other locations were also compared and the results (not shown) yielded similar agreement.

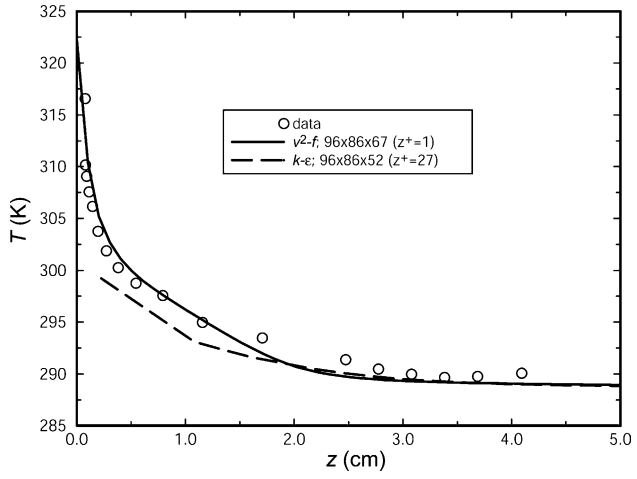

Fig. 6. Temperature profiles normal to surface at $x = 1.64$ m, $y = 1.95$ m; comparison of data and model predictions; forced convection (ID604); $Gr_H/Re_L^2 = 0.18$; $u_\infty = 4.4$ m/s; $T_{w_{avg}} = 323$ K.

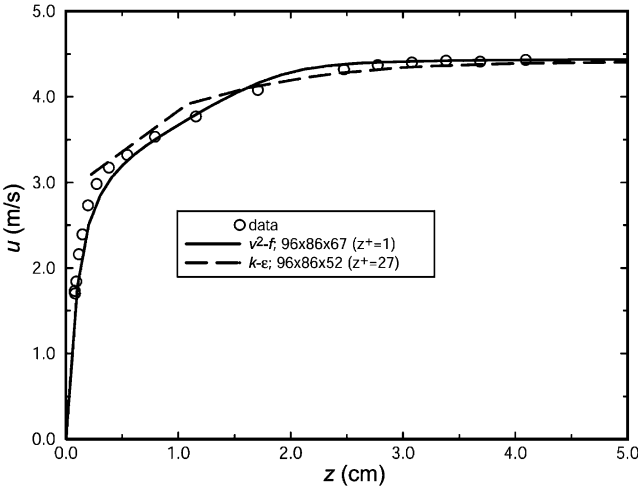

Fig. 7. Horizontal component of velocity profiles normal to surface at $x = 1.64$ m, $y = 1.95$ m; comparison of data and model predictions; forced convection (ID604); $Gr_H/Re_L^2 = 0.18$; $u_\infty = 4.4$ m/s; $T_{w_{avg}} = 323$ K.

4.2. Natural convection ($Gr_H/Re_L{}^2 = \infty$, $Gr_H = 1.42 \times 10^{12}$)

The heat transfer coefficient data of Siebers (1983) and the results from the $\overline{v^2}$–f and k–ε turbulence models are shown in Fig. 8 for the natural convection condition. The average experimental surface and free-stream temperatures are 698 K and 294 K, respectively. In the vertical direction, away from the bottom leading edge of the surface the heat transfer coefficient data are essentially independent of distance. Henkes (1990) and Lin and Churchill (1978) have shown that several versions of the k–ε model result in an increase of h with increasing distance. The present calculations for both the k–ε and the $\overline{v^2}$–f models also show an increase of h with distance

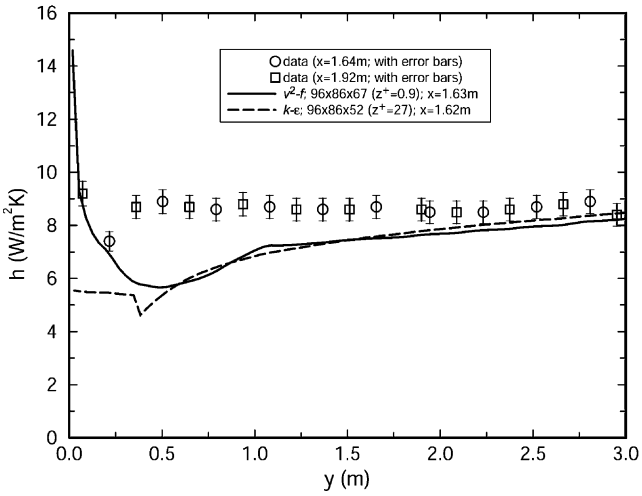

Fig. 8. Variation of local heat transfer coefficient with vertical position on surface at horizontal location $x = 1.6$ m; natural convection (ID643); $T_{w_{avg}} = 698$ K.

in Fig. 8. The $\overline{v^2}$–f model results shown are for a mesh of $96 \times 86 \times 67$, resulting in $z^+ \approx 0.9$ for the first mesh point away from the wall. A calculation (not shown) on a mesh of $67 \times 60 \times 47$ (with $z^+ \approx 1.2$ for the first mesh point away from the wall) yielded a local heat transfer coefficient that agreed to within 1% with the $\overline{v^2}$–f model results shown in Fig. 8. Similarly a k–ε model calculation (not shown) on a mesh of $67 \times 60 \times 52$ yielded a local heat transfer coefficient that agreed to within 1% with the k–ε model results shown in Fig. 8.

4.3. Mixed convection ($Gr_H/Re_L^2 = 2.32 \times 10^{12}/(8.7 \times 10^5)^2 = 3.06$)

The heat transfer coefficient data of Siebers (1983) and the results from the $\overline{v^2}$–f and k–ε turbulence models are shown along a horizontal line at $y = 1.55$ m and along a vertical line at $x = 2.76$ m in Figs. 9 and 10, respectively. The free-stream (and inlet at $x = 0$) velocity and temperature are 4.33 m/s and 289 K, respectively; the average surface temperature is 829 K. In the horizontal direction (Fig. 9), away from the vertical leading edge, the data for h decrease slowly with distance. The $\overline{v^2}$–f model results show a similar trend with distance downstream of transition. The k–ε model results show a transition-like behavior over most of the surface. The $\overline{v^2}$–f model results are in better agreement with the data for this condition.

Note that in comparing Fig. 5 (forced convection) and Fig. 9 (mixed convection) both the data and the model results show a smaller heat transfer coefficient for mixed convection in comparison to forced convection (the free-stream velocities are approximately the same for both cases; 4.33 m/s for the mixed convection case and 4.4 m/s for the forced convection case). This

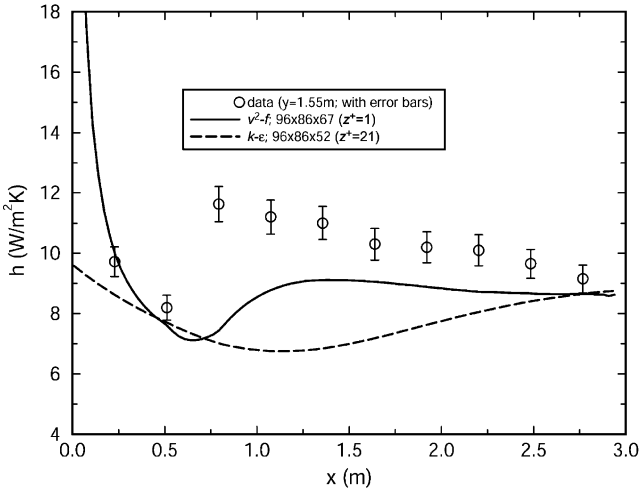

Fig. 9. Variation of local heat transfer coefficient in horizontal direction on surface at vertical location $y = 1.55\,\text{m}$; mixed convection (ID648); $Gr_H/Re_L^2 = 3.06$; $u_\infty = 4.33\,\text{m/s}$; $T_{w_{avg}} = 829\,\text{K}$.

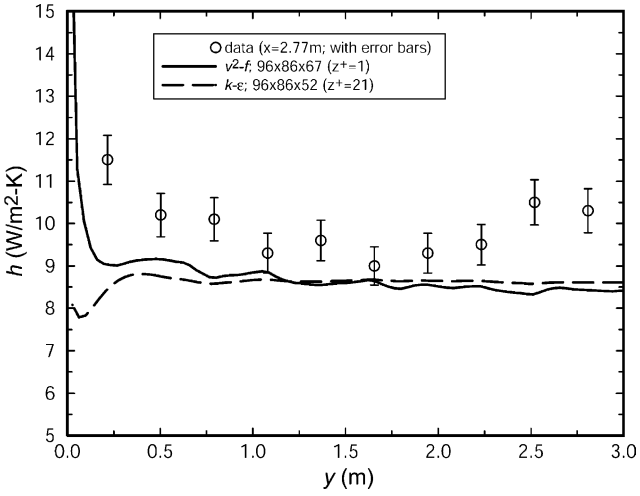

Fig. 10. Variation of local heat transfer coefficient in vertical direction on surface at horizontal location $x = 2.76\,\text{m}$; mixed convection (ID648); $Gr_H/Re_L^2 = 3.06$; $u_\infty = 4.33\,\text{m/s}$; $T_{w_{avg}} = 829\,\text{K}$.

trend in the heat transfer, however, is not necessarily true for all of the cases studied experimentally by Siebers (1983); i.e., for some cases the heat transfer for mixed convection is greater than that for forced convection. For some cases studied by Siebers the flow was transitional over much of the surface. We note that there are complex effects resulting from both variable properties and buoyancy and indeed there are cases (not shown) where there is a larger heat transfer coefficient for mixed convection in comparison to forced convection.

In the vertical direction (Fig. 10), away from the bottom leading edge of the surface the heat transfer coefficient data show some scatter. Based on all of his data in the mixed convection region, Siebers (1983) states that the data for h show little vertical dependence which is in agreement with the calculations for the $\overline{v^2}$–f and k–ε models.

Profiles of temperature and the horizontal and vertical components of velocity normal to the surface at two locations ($x = 2.76\,\text{m}$, $y = 0.22\,\text{m}$; $x = 2.76\,\text{m}$, $y = 2.52\,\text{m}$) are shown in Figs. 11–13, respectively.

The profiles are predicted fairly well although both models over-predict the measured horizontal component of velocity near the lower edge of the surface (Fig. 12 for $y = 0.22\,\text{m}$). The k–ε model significantly under-predicts the measured vertical component of velocity near the upper edge of the surface (Fig. 13 for $y = 2.52\,\text{m}$).

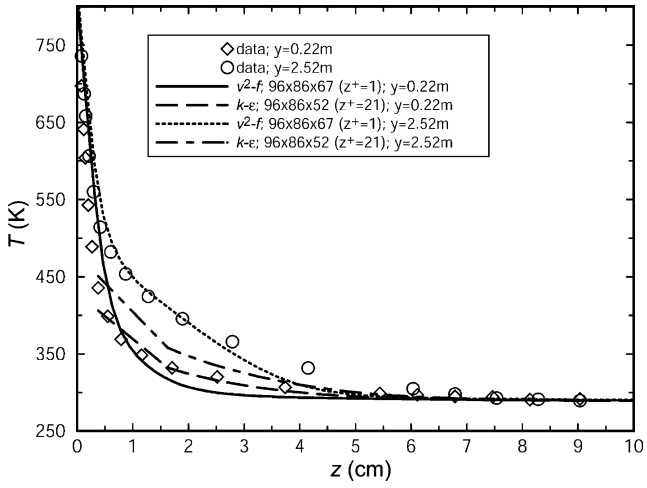

Fig. 11. Temperature profiles normal to the surface at $x = 2.76$ m ($y = 0.22\,\text{m}$, $2.52\,\text{m}$); comparison of data and model predictions; mixed convection (ID648); $Gr_H/Re_L^2 = 3.06$; $u_\infty = 4.33\,\text{m/s}$; $T_{w_{avg}} = 829\,\text{K}$.

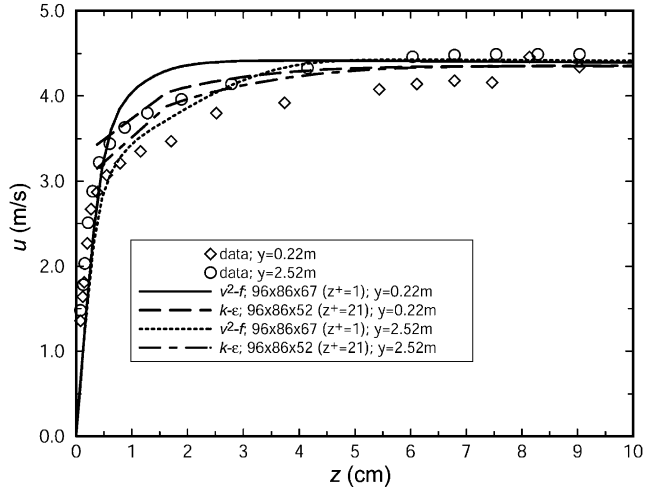

Fig. 12. Horizontal component of velocity profiles normal to the surface at $x = 2.76\,\text{m}$ ($y = 0.22\,\text{m}$, $2.52\,\text{m}$); comparison of data and model predictions; mixed convection (ID648); $Gr_H/Re_L^2 = 3.06$; $u_\infty = 4.33\,\text{m/s}$; $T_{w_{avg}} = 829\,\text{K}$.

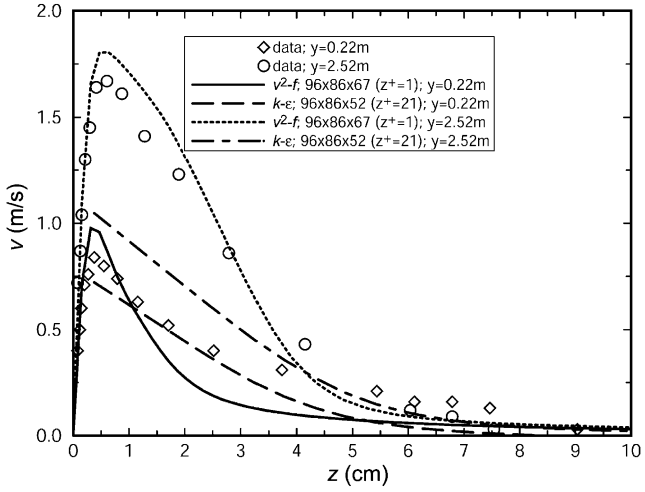

Fig. 13. Vertical component of velocity profiles normal to the surface at $x = 2.76$ m ($y = 0.22$ m, 2.52 m); comparison of data and model predictions; mixed convection (ID648); $Gr_H/Re_L^2 = 3.06$; $u_\infty = 4.33$ m/s; $T_{w_{avg}} = 829$ K.

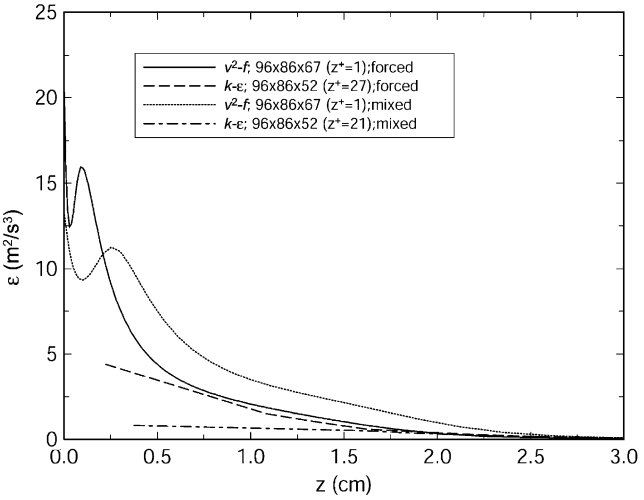

Fig. 15. Calculated turbulent dissipation rate profiles normal to the surface at $x = 1.64$ m, $y = 1.95$ m, for the $\overline{v^2}$–f and k–ε models for forced (ID604 $Gr_H/Re_L^2 = 0.18$; $u_\infty = 4.4$ m/s; $T_{w_{avg}} = 323$ K) and mixed (ID648; $Gr_H/Re_L^2 = 3.06$; $u_\infty = 4.33$ m/s; $T_{w_{avg}} = 829$ K) convection.

Profiles of turbulence quantities, k, ε, and μ_t normal to the surface at the location $x = 1.64$ m, $y = 1.95$ m, calculated using the $\overline{v^2}$–f and k–ε models, are shown for the forced and mixed convection cases in Figs. 14–16, respectively. Both models predict reduced levels of k and ε close to the surface for mixed convection compared to forced convection. Farther from the surface (outside the peak in k) the $\overline{v^2}$–f model results show increased levels of k and ε for mixed convection compared to forced convection. For the k–ε model, outside the peak in k, the level of k is only slightly larger for mixed convection and ε is smaller throughout the boundary layer for mixed convection compared to forced convection (cf. Fig. 15). The calculated turbulent viscosity profiles in Fig. 16 show only slight differences for these two conditions with the k–ε model. For the $\overline{v^2}$–f model, Fig. 16 shows that the turbulent viscosity μ_t is at first smaller for mixed convection compared to forced convection and then larger as the distance from the surface increases.

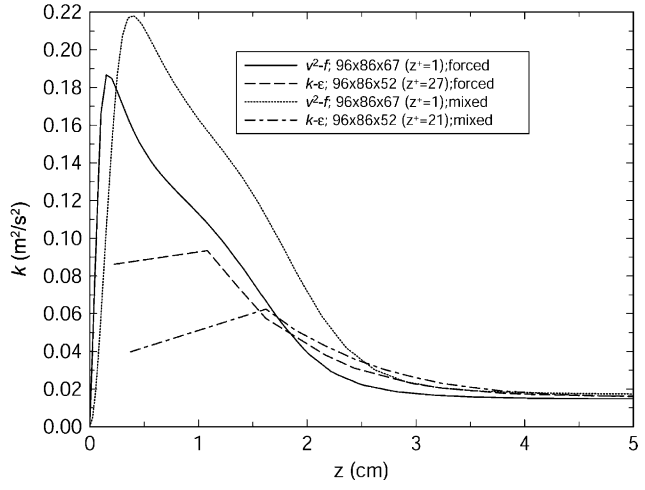

Fig. 14. Calculated turbulent kinetic energy profiles normal to the surface at $x = 1.64$ m, $y = 1.95$ m, for the $\overline{v^2}$–f and k–ε models for forced (ID604 $Gr_H/Re_L^2 = 0.18$; $u_\infty = 4.4$ m/s; $T_{w_{avg}} = 323$ K) and mixed (ID648; $Gr_H/Re_L^2 = 3.06$; $u_\infty = 4.33$ m/s; $T_{w_{avg}} = 829$ K) convection.

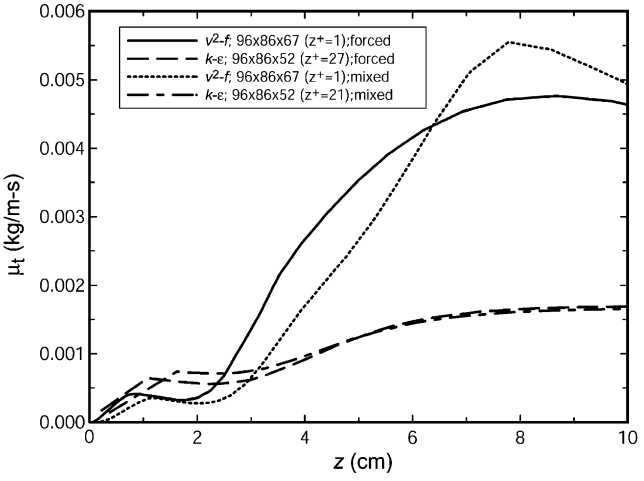

Fig. 16. Calculated turbulent viscosity profiles normal to the surface at $x = 1.64$ m, $y = 1.95$ m, for the $\overline{v^2}$–f and k–ε models for forced (ID604 $Gr_H/Re_L^2 = 0.18$; $u_\infty = 4.4$ m/s; $T_{w_{avg}} = 323$ K) and mixed (ID648; $Gr_H/Re_L^2 = 3.06$; $u_\infty = 4.33$ m/s; $T_{w_{avg}} = 829$ K) convection.

For these cases the smaller values of the turbulence quantities near the surface in mixed convection compared to forced convection predicted by the $\overline{v^2}$–f model may contribute to the reduction in heat transfer coefficient. Other factors such as variable properties and buoyancy-generated vorticity in opposition to shear-generated vorticity may also be affecting the heat transfer at higher surface temperatures.

5. Summary and conclusions

Turbulent, three-dimensional, mixed convection heat transfer from a large (3 m square) vertical flat surface at high temperatures is studied. Results of heat transfer and velocity and temperature profiles of two RANS turbulence models: a standard k–ε model and the $\overline{v^2}$–f model, are compared with experimental data for three cases that span the range covered in the experiment from forced ($Gr_H/Re_L^2 = 0.18$) to mixed ($Gr_H/Re_L^2 = 3.06$) to natural ($Gr_H/Re_L^2 = \infty$) convection. Calculated profiles of turbulence quantities for the two models are presented at a selected point on the surface and compared for forced and mixed convection. For the forced and mixed convection cases, the experimental heat transfer coefficient shows a transition from laminar to turbulent flow, followed by a gradual decrease in the heat transfer coefficient with distance downstream of the vertical leading edge. Although no attempt was made to model transition, the heat transfer coefficients calculated by both models show a transition-like behavior, even though the models assumed turbulent flow at the leading edges of the surface. Both experimental data and model results show a decrease in the heat transfer coefficient as the mixed convection parameter is increased from 0.18 (forced convection) to 3.06 (mixed convection), for approximately the same free-stream velocity (4.4 m/s). In the natural convection case the experimental heat transfer coefficient is approximately constant in the region where the flow is turbulent over the surface, whereas the calculated heat transfer coefficients from both models show a slight increase with vertical distance from the lower (horizontal) edge of the surface. For the three cases studied, which span the range of parameters of the experiment, the calculated local heat transfer coefficients of both models agree with the data to within 5–35% over most of the vertical surface. Profiles of calculated temperature and horizontal and vertical components of velocity at several locations on the surface are compared with experimental data. The agreement is very good for the $\overline{v^2}$–f model and reasonably good for the k–ε model. Calculated turbulence profiles at a selected point on the surface for the k–ε model show little difference between the forced and mixed convection cases studied; for the $\overline{v^2}$–f model the results show reduced levels of turbulence near the surface and enhanced levels away from the surface for the mixed convection case compared with the forced convection case.

Acknowledgments

We wish to acknowledge Professor W. P. Jones of Imperial College of Science, Technology, and Medicine and Professor P. Durbin and Dr. G. Iaccarino of Stanford University for helpful discussions on turbulence transport and the $\overline{v^2}$–f turbulence model. We also wish to acknowledge Chris Moen and Stefan Domino of the Fuego development team for assistance with model implementation and post processing of results.

References

Abu-Mulaweh, H.I., Chen, T.S., Armaly, B.F., 2000. Effects of free-stream velocity on turbulent natural convection flow along a vertical plate. Exp. Heat Transfer 13, 183–195.

Abu-Mulaweh, H.I., Armaly, B.F., Chen, T.S., 2001. Turbulent mixed convection flow over a backward-facing step. Int. J. Heat Mass Transfer 44 (14), 2661–2669.

Afshari, B., 1989. Computation of Three-dimensional Turbulent mixed Convection Boundary Layers. PhD thesis, Stanford University.

Armaly, B.F., Li, A., Abu-Mulaweh, H.I., Chen, T.S., 2000. Measurements and predictions of turbulent natural convection adjacent to backward-facing step. J. Thermophys. Heat Transfer 14 (4), 584–592.

Behnia, M., Parneix, S., Shabany, Y., Durbin, P.A., 1999. Numerical study of turbulent heat transfer in confined and unconfined impinging jets. Int. J. Heat Fluid Flow 20, 1–9.

Chen, T.S., Armaly, B.F., Ali, M.N., 1987. Turbulent mixed convection along a vertical plate. J. Heat Transfer 109 (1), 251–253.

Durbin, P.A., 1991. Near-wall turbulence closure modeling without "damping functions". Theor. Comput. Fluid Dyn. 3, 1–13.

Durbin, P.A., 1993. Application of a near-wall turbulence model to boundary layers and heat transfer. Int. J. Heat Fluid Flow 14 (4), 316–323.

Durbin, P.A., 1996. On the k–ε stagnation point anomaly. Int. J. Heat Fluid Flow 17 (1), 89–90.

Durbin, P.A., 2003. Personal communication.

Hattori, Y., Tsuji, T., Nagano, Y., Tanaka, N., 2000. Characteristics of turbulent combined-convection boundary layer along a vertical heated plate. Int. J. Heat Fluid Flow 21, 520–525.

Hattori, Y., Tsuji, T., Nagano, Y., Tanaka, N., 2001. Effects of freestream on turbulent combined-convection boundary layer along a vertical heated plate. Int. J. Heat Fluid Flow 22, 315–322.

Henkes, R.A.W.M., 1990. Natural Convection Boundary Layers. PhD thesis, Delft University.

Humphrey, J.A.C., To, W.M., 1986. Numerical simulation of buoyant turbulent flow. Part II: free and mixed convection in heated cavities. Int. J. Heat Mass Transfer 29, 593–610.

Jones, W.P., Launder, B.E., 1972. The prediction of laminarization with a two-equation model of turbulence. Int. J. Heat Mass Transfer 15, 301–314.

Kee, R.J., Dixon-Lewis, G., Warnatz, J., Coltrin, M.E., Miller, J.A., 1991. A fortran computer code package for the evaluation of gas-phase multicomponent transport properties. Sandia National Laboratories Report SAND86-8246.

Kee, R.J., Rupley, F.M., Meeks, E., Miller, J.A., 1996. CHEMKIN-III: a fortran chemical kinetics package for the analysis of gas-phase chemical and plasma kinetics. Sandia National Laboratories Report SAND96-8216.

Kitamura, K., Inagaki, T., 1987. Turbulent heat and momentum transfer of combined forced and natural convection along a vertical flat plate-aiding flow. Int. J. Heat Mass Transfer 30 (1), 23–41.

Launder, B.E., Spalding, D.B., 1974. The numerical computation of turbulent flows. Comput. Meth. Appl. Mech. Eng. 3, 269–289.

Li, A., Zhao, J.Z., Chen, T.S., Armaly, B.F., 1998. The effect of forced flow on turbulent natural convection adjacent to a vertical backward-facing step. Heat Transfer 1998, Proc. 11th Int. Heat Transfer Conf., Kyongju, Korea, 3 August 23–28, pp. 269–274.

Lin, S.-J., Churchill, S.W., 1978. Turbulent free convection from a vertical, isothermal plate. Numer. Heat Transfer 1, 129–145.

Moen, C.D., Evans, G.H., Domino, S.P., Burns, S.P., 2002. A multi-mechanics approach to computational heat transfer. IMECE2002-33098, Proc. 2002 ASME Int. Mechanical Eng. Congress and Exhibition, New Orleans, November, pp. 17–22.

Ramachandran, N., Armaly, B.F., Chen, T.S., 1990. Turbulent mixed convection over an isothermal horizontal flat-plate. J. Heat Transfer 112 (1), 124–129.

Seo, E.R., Parameswaran, S., 2000. Buoyant effects on fluid flow and heat transfer in separating flows. FEDSM2000-11222, Proc. 2000 ASME Fluids Eng. Div. Summer Meeting, Boston, June 11–15.

Siebers, D.L., 1983. Experimental Mixed Convection Heat Transfer from a Large, Vertical Surface in a Horizontal Flow. PhD thesis, Stanford University.

Siebers, D.L., Schwind, R.G., Moffat, R.F., 1982. Experimental mixed convection from a large, vertical plate in a horizontal flow. Paper MC13, vol. 3, Proc. 7th Int. Heat Transfer Conf., Munich, 1982.

Siebers, D.L., Moffat, R.F., Schwind, R.G., 1985. Experimental, variable properties natural convection from a large, vertical flat surface. J. Heat Transfer 107 (February), 124–132.

Sveningsson, A., 2003. Analysis of the Performance of Different $\overline{v^2}$–f Turbulence Models in a Stator Vane Passage Flow. PhD thesis, Chalmers University of Technology.